JOURNAL OF Applied Polymer SCIENCE

Development of Optically Transparent ZnS/Poly(vinylpyrrolidone) Nanocomposite Films with High Refractive Indices and High Abbe Numbers

Quanyuan Zhang,[1] Eunice Shing Mei Goh,[2] Roger Beuerman,[3] Zaher Judeh,[1] Mary B. Chan-Park,[1] Tupei Chen,[2] Rong Xu[1]

[1]School of Chemical & Biomedical Engineering, Nanyang Technological University, N1.2, 62 Nanyang Drive, Singapore 637459, Singapore

[2]School of Electrical and Electronic Engineering, Nanyang Technological University, Singapore 639798, Singapore

[3]Singapore Eye Research Institute, 11 Third Hospital Ave 168751, Singapore 6223 8458, Singapore

Correspondence to: R. Xu (E-mail: rxu@ntu.edu.sg)

ABSTRACT: A series of optically transparent ZnS-poly(vinylpyrrolidone) (PVP) nanocomposite films with high refractive indices and high Abbe numbers have been prepared. Mercaptoethanol (ME) capped ZnS nanoparticles (NPs) were introduced into the PVP polymer matrix via simple blending with high nanophase contents. ME-ZnS NPs of around 3 nm were prepared from zinc acetate and thiourea precursors in *N*,*N*-dimethylformamide using ME as a capping agent. Transparent nanocomposite films with high refractive indices and high Abbe numbers can be easily prepared by a conventional film casting method. TGA results indicated that the ZnS/PVP nanocomposite films exhibit good thermal stability and the measured contents of ZnS NPs in the films agree well with the theoretical values. The refractive indices and the Abbe numbers of the ZnS/PVP nanocomposite films range from 1.5061 to 1.7523 and 55.6 to 20.4 with the content of ME-ZnS NPs varied between 0 and 80 wt %, respectively. © 2012 Wiley Periodicals, Inc. J. Appl. Polym. Sci. 129: 1793–1798, 2013

KEYWORDS: composites; films; nanoparticles; nanowires and nanocrystals; optical properties; properties and characterization

Received 13 July 2012; accepted 27 November 2012; published online 22 December 2012
DOI: 10.1002/app.38883

INTRODUCTION

Recently, functional optical materials with both high refractive indices (n_D) and high Abbe numbers (v_D) have attracted significant interest owing to their potential applications in ophthalmic lenses, prisms, optical waveguides, and diffractive grating.[1–6] Among various physical properties required for optical material applications, transparency, refractive index (n_D), and Abbe number (v_D) are three primary parameters. For example, high refractive index materials when used as lens can yield a relatively thinner lens optic in order to achieve the proper refractive power as that of low refractive index materials. The Abbe number (v_D), which is a main parameter for refractive index dispersion and is described by the following equation:

$$v_D = (n_D - 1)/(n_F - n_C) \quad (1)$$

where n_D, n_F, and n_C are the refractive indices of the material at the wavelengths of the spectral lines of sodium D (589.3 nm), hydrogen F (486.1 nm), and hydrogen C (656.3 nm), respectively.[7] A larger Abbe number means a lower dispersion in the refractive index.[8] However, for conventional inorganic or organic optical materials, the refractive index and Abbe number relate to each other in such a way that the higher the refractive index, the lower the Abbe's number.[9] Therefore, design and development of optical materials with both high refractive index and high Abbe number remains an important task.

In the past decades, development of optical materials with high refractive indices has received wide attention.[10–14] One of the common approaches is to introduce characteristic substituents such as aromatic rings and sulfur atoms of high molar refractions and low molar volumes to the polymers in order to improve their refractive indices.[15] For example, Takata reported a series of high refractive polyesters[16] and poly(arylene thioether)s[17] by incorporating a fluorene group. Ueda and coworkers[18–22] designed and synthesized a series of sulfur-containing polyimides (PIs). The refractive indices of these PIs ranged from 1.71 to 1.77 at 633 nm and increased with the content of sulfur in the PIs. Another convenient and effective

method of increasing the refractive index of materials is to introduce high refractive index inorganic building blocks such as TiO_2, ZnO, PbS, ZnS, and so forth, into organic matrices at the nanoscale.[23] For instance, Prasad et al. successfully prepared SiO_2/TiO_2/poly(vinylpyrrolidone) (PVP) composite materials with controlled refractive index in the range of 1.49–1.65 at 633 nm by varying the ratio of SiO_2 to TiO_2.[11] Recently, Yang coworkers incorporated ZnS nanoparticles (NPs) into several polymer matrices with high nanophase contents for improving the refractive indices of the nanocomposites.[24–29]

Although many works have been reported on organic–inorganic nanocomposites with high refractive indices, the Abbe numbers of such nanocomposites are quite low or not reported. Wilkes and coworkers developed two series of triethoxysilane capped polymer-titania hybrid materials, poly(arylene ether ketone)-titania (PEK-TiO_2) and poly(arylene ether sulfone)-titania (PES-TiO_2). The refractive indices and the Abbe numbers of these polymer-titania hybrid materials ranged from 1.60–1.75 and 30–20, respectively, with varied TiO_2 contents.[30] Besides increasing the content of the inorganic nanophase, the use of polar organic molecules such as *N*,*N*-dimethylformamide (DMF) and DMAA, which can effectively stabilize and well disperse ZnS NPs due to the coordination interaction between the oxygen atoms of DMF or DMAA and the zinc atoms, has been reported.[26–27,31,32] PVP, which of the repeat unit has a similar molecule structure to DMF or DMAA, can be chosen as the polymer matrix for the dispersion of ZnS NPs due to its good complexation with the metal ions. Although ZnS/PVP nanocomposite suspension and film have been previously investigated, the contents of ZnS NPs in these polymer matrix were quite low and the Abbe number was not reported.[33,34] In this work, we report the synthesis and characterization of a series of optically transparent ZnS/PVP nanocomposite films with high refractive indices and high Abbe numbers via a simple blending method. Such hybrid materials may be found as potential candidates for many optics related applications.

EXPERIMENTAL

Materials

Zinc acetate dihydrate ($Zn(Ac)_2{\cdot}2H_2O$, 98%, Alfa-Aesar), mercaptoethanol (ME, 98%, Alfa-Aesar), thiourea (99%, Alfa-Aesar), PVP (K 90, molecular weight ~360,000, Sigma-Aldrich) and DMF (Fisher Scientific, HPLC grade) were purchased and used without further purification.

Synthesis of ME Capped ZnS NPs

The ME capped ZnS NPs (ME-ZnS) were synthesized in DMF according to a modified literature procedure.[27] $Zn(Ac)_2{\cdot}2H_2O$ (22.0 g, 0.1 mol), ME (11.6 g, 0.148 mol), thiourea (5.5 g, 0.072 mol) and 300 mL of DMF were charged to a 500 mL three-necked round-bottom flask. The flask was equipped with a magnetic stirrer, a condenser and nitrogen purging. The mixture was refluxed at 160°C for 10 h under nitrogen with stirring and then concentrated to 80 mL using a rotary evaporator. The resulting solution was poured into a large amount of ethanol and the white precipitate was collected. The product was washed thoroughly with methanol and then dried in vacuum.

Preparation of Transparent ZnS/PVP Nanocomposite Films

ME-ZnS NPs with desired weight ratio were dispersed in a 10 wt % solution of PVP in DMF. After stirring overnight, the solution was filtered through a 0.2 μm syringe filter to remove the insoluble materials and dust particles. The filtrate was then poured on a leveled clean glass slide. The casting process took about 8 h at 60°C. The resulting films were dried at 80°C for 2 h, 100°C for 2 h, and 120°C for 4 h, respectively.

Characterization Methods

Transmission electron microscopy (TEM) was carried out using a JEOL-3010 microscope with an accelerating voltage of 200 kV. NP samples for TEM were prepared by dispersing a few milligram of the ZnS NPs powder in DMF to form a homogeneous solution and by adding a drop of the solution on the copper grids coated with a carbon film. The X-ray diffraction (XRD) data were collected on a Bruker AXS D8 X-ray diffractometer with a Cu Kα ($\lambda = 1.5406$ Å) source, operated at 40 kV and 20 mA at 293 K. The 2θ scanning range was from 20° to 70° with a step size of 0.02° and at a scanning speed of 1 °/min. Fourier transform infrared-attenuated total reflection (FTIR-ATR) spectra were recorded on a Nicolet Nexus 5700 spectrometer using the Smart Orbit ATR accessory. The beam splitter was KBr and the detector was a liquid nitrogen-cooled MCT detector. For each spectrum, 64 scans were collected at a resolution of 2 cm^{-1}. Thermogravimetric analysis (TGA) was carried out in a PerkinElmer Diamond TG/DTA instrument at a heating rate of 10 °C/min from ambient temperature to 700°C under a flow of nitrogen at 200 mL/min. UV-visible spectra were measured with a SHIMADZU UV-2450 spectrometer in the transmittance mode. The refractive indices of the ZnS/PVP nanocomposite films (on silicon wafer) were measured using a variable angle ellipsometer (J.A.Woollam, Model HS-190) in the wavelength range of 350–1100 nm (i.e., 1.13–3.54 eV) at the incident angle of 75° at room temperature.

RESULTS AND DISCUSSION

Properties of ME Capped ZnS NPs

ME-ZnS NPs synthesized by the current method can be readily dispersed in organic polar solvents such as DMF to obtain stable and transparent solutions with high concentrations. Such characteristics are an essential requirement for the preparation of transparent bulk nanocomposites with NPs individually and uniformed dispersed inside. Figure 1 presents the XRD patterns of ME-ZnS NPs. Because of the formation of nanosized NPs, there are three broad diffraction peaks appearing at around 28.5°, 47.5°, and 56.3° corresponding to the (111), (220), and (311) planes of the zinc blend structure of ZnS (JCPDS No. 05-0566), respectively. The grain size of ZnS NPs was estimated by Scherrer's formula. The average diameter of ME-ZnS NPs was calculated to be about 3.0 nm based on the (111) peak. Such a result is in well agreement with that obtained from TEM. A high resolution TEM image of ME-ZnS NPs is shown in Figure 2. It can be seen that ZnS NPs are well dispersed and they have an average diameter of about 3 nm. The lattice fringes are clearly observed, indicating that the crystallinity of ZnS NPs is good. NPs with good crystallinity are favored over their

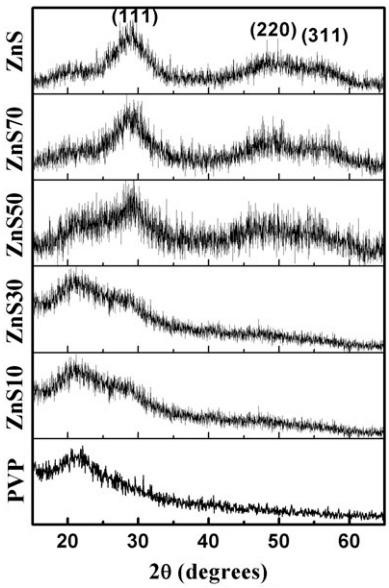

Figure 1. XRD patterns of ME capped ZnS NPs, neat PVP and ZnS/PVP nanocomposites with different ZnS contents.

amorphous counterparts due to the associated higher refractive indices.[35]

Properties of ZnS/PVP Nanocomposite Films

Physical Properties. A series of optically transparent ZnS/PVP nanocomposite films with varied ZnS contents were successfully fabricated by a simple solution casting process after blending ME-ZnS NPs with PVP in DMF solution. The content of ME-ZnS NPs in the PVP matrix ranged from 0 to 80 wt %. PVP can well stabilize and disperse ME-ZnS NPs into the polymer matrix by interacting with the surface of ME-ZnS NPs in two ways: one is complexation with Zn atoms on the surface of ZnS NPs, and the other way is intermolecular hydrogen bonding interaction with hydroxyl of ME molecules on the surface of ZnS NPs, as shown in Scheme 1.

FTIR-ATR spectra of pure PVP and the ZnS/PVP nanocomposite films with different ME-ZnS contents in the range 2000–650 cm^{-1} are shown in Figure 3. The characteristic peaks at 1678 cm^{-1} and 1282 cm^{-1} in the spectrum of pure PVP are assigned to C=O stretching vibration and C—N stretching vibration, respectively.[36] In the spectra of ZnS/PVP nanocomposite films, the characteristic C=O stretching vibration of PVP molecules shifted from 1678 cm^{-1} to a lower wavenumber of around 1654 cm^{-1}. This can be attributed to the intermolecular hydrogen bonding interaction between hydroxyl of ME molecules and carbonyl oxygen of PVP molecules which weakened the force constant of C=O double band.[37] In addition, the peak of C=O stretching vibration gradually shifted to a lower wave number with increasing ZnS content from 10 to 70%, indicating that the formation of stronger intermolecular hydrogen bonding interaction in ZnS/PVP nanocomposite films with higher ZnS nanophase contents.

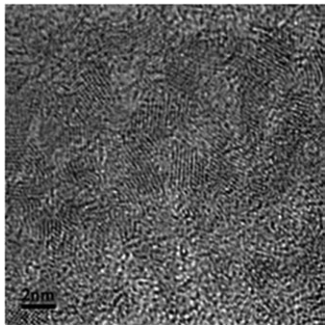

Figure 2. TEM image of ME capped ZnS NPs.

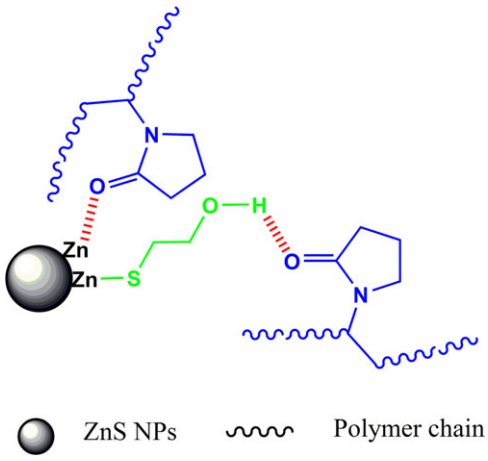

Scheme 1. Schematic illustration of the structure of ZnS/PVP nanocomposite films. [Color figure can be viewed in the online issue, which is available at wileyonlinelibrary.com.]

The wide-angle X-ray diffraction analysis of pure PVP and ZnS/PVP nanocomposite films with different ME-ZnS contents are shown in Figure 1. A broad diffraction band of 2θ at around 21° is associated with the amorphous phase of PVP. All the ZnS/PVP nanocomposite films exhibit three diffraction peaks corresponding to the (111), (220), and (311) planes, which indicates that the zinc blend crystal structure of ZnS NPs did not change in the nanocomposite films. With increasing the

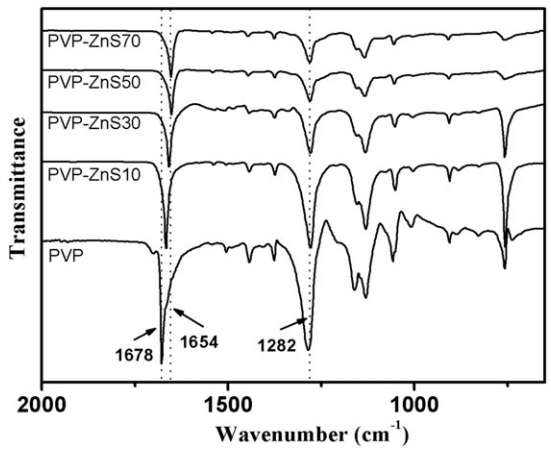

Figure 3. ATR spectra of pure PVP and the ZnS/PVP nanocomposite films with different ZnS contents.

Applied Polymer SCIENCE

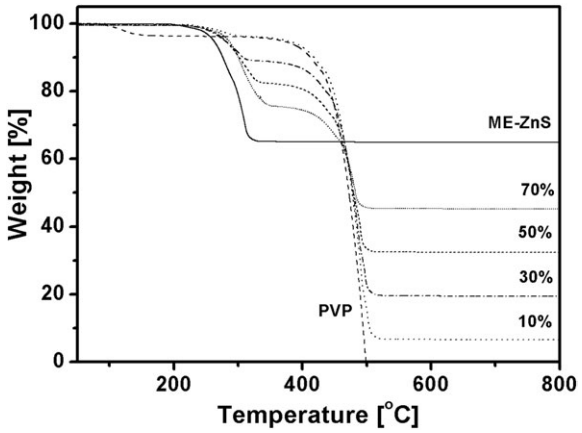

Figure 4. TGA curves of ME capped ZnS NPs, pure PVP and the ZnS/PVP nanocomposites with different ZnS contents.

content of ZnS NPs, the intensities of these diffraction peaks gradually increase and meanwhile the intensities of the diffraction band attributed to PVP gradually decreases, indicating that the ME-ZnS NPs have been successfully incorporated into PVP matrix.

Thermal Properties. The thermal stabilities of the ME-ZnS NPs and ZnS/PVP nanocomposite films with different ME-ZnS contents were studied and their TGA curves are shown in Figure 4. The ME-ZnS NPs started to decompose at about 200°C due to the unstable ME molecules on the surface of ZnS NPs. The decomposition was completed at around 300°C and the residual ZnS contents were about 65 wt % in the ME-ZnS NPs. Such a result indicates that the surface of ZnS is substantially covered by the organic ME molecules. These organic molecules can improve the compatibility of ZnS NPs with the polymer matrix to avoid phase separation. Based on the TGA data, the estimated molar ratio of ME : ZnS is as high as 0.69 : 1.00. The TGA curve for PVP in Figure 4 shows that the PVP matrix began to decompose at about 380°C and decomposed completely without any residue at about 500°C. The thermal stability of the ZnS/PVP nanocomposite films increased a little bit with increasing the content of ME-ZnS NPs. It is interesting to observe that when ME-ZnS NPs were incorporated into the PVP matrix, the decomposition temperature of the ME molecules slightly increases from 200 to 220°C. This is consistent with the formation of the intermolecular hydrogen bonding interaction between ME molecules and PVP matrix in the nanocomposite films. The residues of the nanocomposite films from the TGA curves increase with the increasing ZnS contents. Moreover, these inorganic residue amounts measured are well in accordance with the theoretical amounts of pure ZnS in the ZnS/PVP nanocomposite films, indicating that the different contents of ZnS NPs have been successfully incorporated into the PVP polymer matrix.

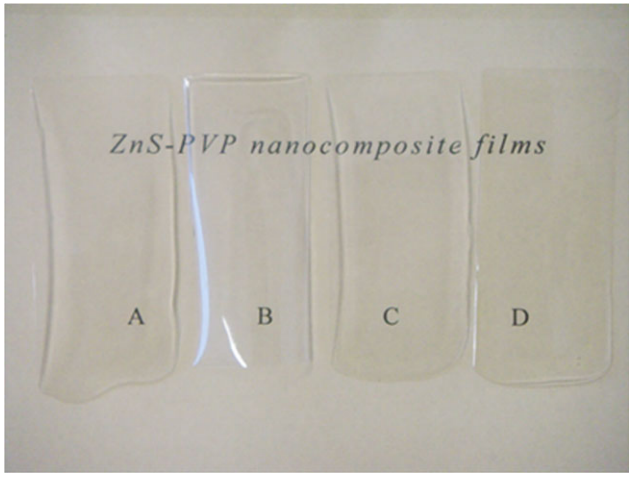

Figure 6. Photograph of the ZnS/PVP nanocomposite films with 50 wt% ME capped ZnS NPs. [Color figure can be viewed in the online issue, which is available at wileyonlinelibrary.com.]

Optical Properties. Transmission UV-vis spectra were measured for the ZnS/PVP nanocomposite films (approximate thickness: 25 μm) with different ZnS contents. Typical UV–vis spectra of some representative nanocomposite films are illustrated in

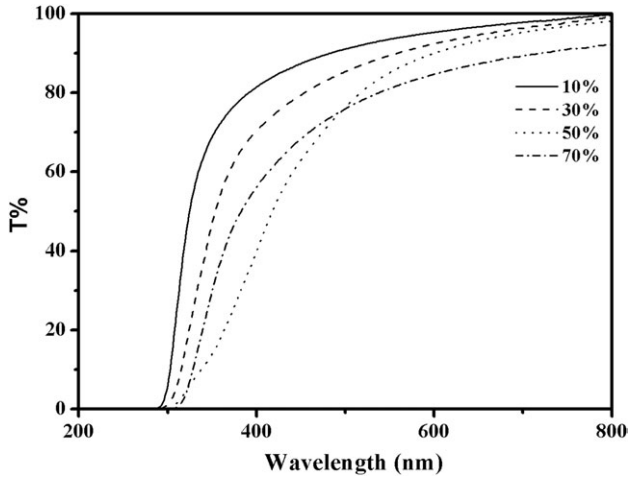

Figure 5. UV-vis transmittance spectra of the ZnS/PVP nanocomposite films with different ZnS contents.

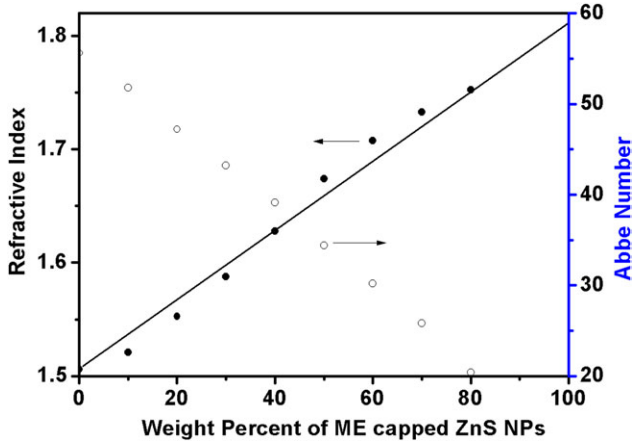

Figure 7. Variation of refractive index and Abbe number with the ME capped ZnS content (wt %). [Color figure can be viewed in the online issue, which is available at wileyonlinelibrary.com.]

Table I. Refractive Indices (n) and Abbe Numbers (ν) of ZnS/PVP Nanocomposite Films with Different ZnS Contents

ME-ZnS (wt %)	0	10	20	30	40	50	60	70	80
n_D ($\lambda = 590$ nm)	1.5061	1.5207	1.5526	1.5875	1.6279	1.6738	1.7076	1.7329	1.7523
ν_D	55.6	51.8	47.2	43.2	39.1	34.4	30.2	25.8	20.4

Figure 5. All the nanocomposite films exhibit good visible light transmittance even when the ME-ZnS content is as high as 80 wt %. The transmittance of all the ZnS/PVP nanocomposite films with different ME-ZnS contents is over 81% at the wavelength of 550 nm. Such results indicate that the ME-ZnS NPs are well dispersed in the films, resulting in good optical homogeneity. Between 325 and 495 nm, transmittance decreases with increasing content of ME-ZnS NPs. The nanocomposite films may scatter and absorb ultraviolet light due to the wide band gap of ZnS, suggesting that they have UV-protection function. Photographs of the ZnS/PVP nanocomposite films with different contents of ME-ZnS NPs are displayed in Figure 6. All the films prepared display to be transparent and clear.

The refractive indices and the Abbe numbers of all the ZnS/PVP nanocomposite films prepared are shown in Figure 7 and the data are summarized in Table I. As the content of ME-ZnS NPs in the PVP matrix increases, the refractive index of the nanocomposite film almost increases linearly from 1.5061 (pure PVP) to 1.7523 (80 wt % ME-ZnS NPs), suggesting that the current approach relying on the interactions between ME-ZnS NPs and PVP matrix (Scheme 1) is effective in enhancing the refractive index of the nanocomposite film. The effect of incorporation of ME-ZnS NPs in the PVP matrix on Abbe number is on a reverse trend, as shown in Figure 7. The Abbe number decreases from 55.6 (pure PVP) to 20.4 (80 wt % ME-ZnS NPs) correspondingly. Our study has shown that ZnS/PVP nanocomposite films of both relatively high refractive indices and Abbe numbers can be obtained by this simple blending method without involving complicated procedures. Further, the content of ZnS can be easily controlled so that the optical properties of the as-prepared ZnS/PVP nanocomposite films can be effectively tuned.

CONCLUSIONS

A series of optically transparent ZnS/PVP nanocomposite films with high refractive indices and high Abbe numbers have been successfully prepared by a solution casting process after blending ME capped ZnS NPs and PVP. All the ZnS/PVP nanocomposite films exhibit good transparency and high thermal stability. The refractive indices and the Abbe numbers of the ZnS/PVP nanocomposite films ranged from 1.5061 to 1.7523 and 55.6 to 20.4, respectively. Such optical properties can be controlled by varying the content of ZnS NPs. The optically transparent nanocomposite films with controlled refractive indices and Abbe numbers could be potentially used as optical thin films for many applications.

ACKNOWLEDGMENTS

This work was supported by National Medical Research Council (Grant number: NMRC/NIG/0022/2008) and SingHealth Foundation (Grant number: SHF/09/GMC(1)/012(R)), Singapore.

REFERENCES

1. Suzuki, Y.; Higashihara, T.; Ando, S.; Ueda, M. *Eur. Polym. J.* **2010**, *46*, 34.
2. Suzuki, Y.; Higashihara, T.; Ando, S.; Ueda, M. *Polym. J.* **2009**, *41*, 860.
3. Okutsu, R.; Ando, S.; Ueda, M. *Chem. Mater.* **2008**, *20*, 4017.
4. Okutsu, R.; Suzuki, Y.; Ando, S.; Ueda, M. *Macromolecules* **2008**, *41*, 6165.
5. Gao, C. L.; Yang, B.; Shen, J. C. *J. Appl. Polym. Sci.* **2000**, *75*, 1474.
6. Matsuda, T.; Funae, Y.; Yoshida, M.; Yamamoto, T.; Takaya, T. *J. Appl. Polym. Sci.* **2000**, *76*, 50.
7. Okubo, T.; Kohmoto, S.; Yamamoto, M. *J. Macromol. Sci. Pure Appl. Chem.* **1998**, A35, 1819.
8. Dislich, H. *Angew. Chem. Int. Ed. Engl.* **1979**, *18*, 49.
9. Yang, C. J.; Jenekhe, S. A. *Chem. Mater.* **1995**, *7*, 1276.
10. Nakayama, N.; Hayashi, T. *Prog. Org. Coat.* **2008**, *62*, 274.
11. Bae, W. J.; Trikeriotis, M.; Sha, J.; Schwartz, E. L.; Rodriguez, R.; Zimmerman, P.; Giannelis, E. P.; Ober, C. K. *J. Mater. Chem.* **2010**, *20*, 5186.
12. Liu, J. G.; Ueda, M. *J. Mater. Chem.* **2009**, *19*, 8907.
13. Lü, C. L.; Yang, B. *J. Mater. Chem.* **2009**, *19*, 2884.
14. Simmrock, H. U.; Mathy, A.; Dominguez, L.; Meyer, W. H.; Wegner, G. *Adv. Mater.* **1989**, *8*, 294.
15. Yang, C. J.; Jenekhe, S. A. *Chem. Mater.* **1995**, *7*, 1276.
16. Seesukphronrarak, S.; Kawasaki, S.; Kobori, K.; Takata, T. *J. Polym. Sci. Part A: Polym. Chem.* **2008**, *46*, 2549.
17. Seesukphronrarak, S.; Kawasaki, S.; Kobori, K.; Takata, T. *J. Polym. Sci. Part A: Polym. Chem.* **2007**, *45*, 3073.
18. Fukuzaki, N.; Higashihara, T.; Ando, S.; Ueda, M. *Macromolecules* **2010**, *43*, 1836.
19. You, N. H.; Sukuzi, Y.; Higashihara, T.; Ando, S.; Ueda, M. *Polymer* **2009**, *50*, 789.
20. Liu, J. G.; Nakamura, Y.; Shibasaki, Y.; Ando, S.; Ueda, M. *J. Polym. Sci. Part A: Polym. Chem.* **2007**, *45*, 5606.
21. Liu, J. G.; Nakamura, Y.; Shibasaki, Y.; Shibasaki, Y.; Ando, S.; Ueda, M. *Macromolecules* **2007**, *40*, 7902.
22. Liu, J. G.; Nakamura, Y.; Shibasaki, Y.; Shibasaki, Y.; Ando, S.; Ueda, M. *Macromolecules* **2007**, *40*, 4614.
23. Yoshida, M.; Prasad, P. N. *Chem. Mater.* **1996**, *8*, 235.
24. Lin, Z.; Cheng, Y. R.; Lü, H.; Zhang, L.; Yang, B. *Polymer* **2010**, *51*, 5424.
25. Guan, C.; Lü, C. L.; Cheng, Y. R.; Song, S. Y.; Yang, B. *J. Mater. Chem.* **2009**, *19*, 617.

26. Cheng, Y. R.; Lü, C. L.; Lin, Z.; Liu, Y. F.; Guan. C.; Lü, H.; Yang, B. *J. Mater. Chem.* **2008**, *18*, 4062.
27. Lü, C. L.; Cheng, Y. R.; Liu, Y. F.; Liu, F.; Yang, B. *Adv. Mater.* **2006**, *18*, 1188.
28. Lü, C. L.; Cui, Z. C.; Wang, Y.; Li, Z.; Guan, C.; Yang, B.; Shen, J. C. *J. Mater. Chem.* **2003**, *13*, 2189.
29. Lü, C. L.; Cui, Z. C.; Li, Z.; Yang, B.; Shen, J. C. *J. Mater. Chem.* **2003**, *13*, 526.
30. Wang, B.; Wilkes, G. L.; Hedrick, J. C.; Liptak, S. C.; McGrath, J. E. *Macromolecules* **1991**, *24*, 3449.
31. HosoKawa, H.; Murakoshi, K.; Wada, Y.; Yanagida, S.; Satoh, M. *Langmuir* **1996**, *12*, 3598.
32. HosoKawa, H.; Fujiwara, H.; Murakoshi, K.; Wada, Y.; Yanagida, S.; Satoh, M. *J. Phys. Chem.* **1996**, *100*, 6649.
33. Wang, C. X.; Guan, L. S.; Mao, Y. L.; Gu, Y. Z.; Liu, J. H.; Fu, S. S.; Xu, Q. H. *J. Phys. D. Appl. Phys.* **2009**, *42*, 045403.
34. Ullah, M. H.; Kim, J. H.; Ha, C. S. *Mater. Lett.* **2008**, *62*, 2249.
35. Papadimitrakopoulos, F.; Wisniecki P.; Bhagwagar, E. D. *Chem. Mater.* **1997**, *9*, 2928.
36. Sui, X. M.; Liu, Y. C.; Shao, C. L.; Liu, Y. X.; Xu, C. S. *Chem. Phys. Lett.* **2006**, *424*, 340.
37. Zhang, Q.; Zhang, T. R.; Ge, J. P.; Yin, Y. D. *Nano Lett.* **2008**, *8*, 2867.